Dynamics in a supercooled molecular liquid: Theory and simulations

Adele Rinaldi, Francesco Sciortino, and Piero Tartaglia

Dipartimento di Fisica and Istituto Nazionale per la Fisica della Materia, Università di Roma La Sapienza, Piazzale Aldo Moro 2, I-00185, Roma, Italy

We report extensive simulations of liquid supercooled states for a simple three-site molecular model, introduced by Lewis and Wahnström [Phys. Rev. E **50**, 3865 (1994)] to mimic the behavior of *ortho*-terphenyl. The large system size and the long simulation length allow us to calculate very precisely (in a large q-vector range) self-correlation and collective correlation functions, providing a clean and simple reference model for theoretical descriptions of molecular liquids in supercooled states. The time and wave-vector dependence of the site-site correlation functions are compared (neglecting the molecular constraints) with detailed ideal mode-coupling theory predictions. Except for the wave-vector region where the dynamics are controlled by the center of mass (around 9 nm^{-1}), the theoretical predictions compare very well with the simulation data.

I. INTRODUCTION

In the last decade, increased computational resources have been used to tackle the study of the onset of glassy dynamics [1–8], one of the most interesting open problems in the physics of liquids. Supercooled liquids are indeed characterized by an extreme T dependence of the structural times, which covers more than 15 orders of magnitude in a small temperature interval. Present computer facilities allow one to follow the change in the structure and in the dynamics of the system (in equilibrium) over a T range where the diffusivity changes by more than five orders of magnitude. At the same time, computer simulations are starting to provide a detailed picture of the structure of the potential energy landscape probed in supercooled states [9–14]. The calculated trajectories offer an outstanding possibility for studying the origin of the slowing down of the dynamics, and call for a careful comparison between theories and ''exact'' numerical calculations.

Exact results calculated for model-system and theoretical predictions based on mode coupling theory (MCT) [15,16] have been reported for several atomic liquids, encompassing hard spheres, soft spheres, Lennard-Jones potentials [2], and recently silica [17]. In the case of molecular liquids, where the possibility of comparing with experiments makes the effort even more valuable, molecular dynamics (MD) simulations extending to the 100-ns time scale are now possible. Detailed comparisons between theories and simulations appear as well [18–21].

MD simulations have often been used to generate reference systems for validating theories of liquids, starting from the pioneering work of Alder and Wainwright [22] on hard spheres. A very interesting model for a molecular liquid was designed by Lewis and Wahnström (LW) [23] by gluing three identical Lennard-Jones (LJ) atoms in a rigid molecule. The shape of the molecule (an isosceles triangle) and the LJ parameters were chosen to mimic as closely as possible one of the most studied glass-forming liquid [24–31] *ortho*-terphenyl (OTP). This model provides a clean bridge between studies based on atomic LJ potentials and more complex molecular potentials. From a theoretical point of view,

such a model is also very valuable, since the LW model lends itself to several approximations of increasing complexity. For example, one could consider the LW system as a liquid of identical sites, correlated in space according to the site-site correlation function (without differentiating between intramolecular and intermolecular sites), or one can improve by including the molecular correlation via the triplet site-site-site correlations. A theoretical study of the dynamics for this molecular model, implementing a full site-site description [32] or an expansion in generalized spherical harmonics [33,34], to account for the intramolecular constraints, is also foreseeable.

The LW potential was introduced in Ref. [23]. Self and collective properties of this model in weakly supercooled states were studied and discussed. In a following paper [35], LW reported some preliminary attempts to describe the intermediate time dynamics using MCT predictions. Favored by the increased computational power, we have decided to revisit such a model and—by extending the simulation time by a factor 20 and the number of molecules by a factor 30—to calculate detailed properties of the dynamics in supercooled states, like the nonergodicity parameters for both self, collective, and orientational properties to be used as reference system to be compared with theoretical predictions. We present such data in this paper. We also solve the MCT equations for such a model, using as input the site-site structure factor and the site-site-site triplet correlation functions calculated from the simulated trajectories. The comparison between the molecular dynamics data and the MCT predictions is very valuable in assessing the role of the center of mass dynamics (which is neglected in the chosen MCT approach), the role of the triplet correlations [36,17] and, in general, the ability of ideal MCT to capture the dynamics of molecular liquids in weakly supercooled states.

II. MODEL AND NUMERICS

The geometry of the LW molecule is a rigid three site isosceles triangle hosting a Lennard-Jones atom on each site. The site-site spherical potential is

TABLE I. For each temperature, the diffusion coefficient, the density, the average potential energy, the pressure, and the length of the simulation time after equilibration are reported.

T (K)	D (10^{-5} cm^2/s)	ρ (g/cm^3)	U (kJ/mol)	P (MPa)	t_{sim} (ns)
255	0.000 35	1.0851	-77.6	0.02	41
260	0.0010	1.0822	-77.3	-1.2	52
266	0.0020	1.0790	-77.0	-1.0	37
275	0.0043	1.0763	-76.5	5.4	37
281	0.012	1.0703	-75.8	0.7	14
291	0.025	1.0650	-75.2	2.0	16
305	0.059	1.0554	-74.1	1.0	5
318	0.12	1.0439	-72.9	-2.3	7
346	0.25	1.0269	-71.0	-13.0	6

$$V(r) = 4\epsilon \left[\left(\frac{\sigma}{r} \right)^{12} - \left(\frac{\sigma}{r} \right)^{6} \right] + A + Br, \tag{1}$$

with $\epsilon = 5.276$ kJ/mol, $\sigma = 0.4828$ nm, $A = 0.4612$ kJ/mol, and $B = -0.3132$ (kJ/mol)/nm. The parameters of the potential have been selected to reproduce bulk properties of the OTP molecule [23]. The values of A and B have been selected to bring the potential and its first derivative to zero at $r = 1.2616$ nm. The resulting potential has a minimum at $r = 0.5421$ nm of depth -4.985 kJ/mol. The length of the two short sides is 0.483 nm, and that of the long side 0.588 nm, forming an isosceles angle of $75°$.

We have studied a system composed by $N = 9261$ molecules for several state points, from $T = 255$ to 346 K, as listed in Table I. The choice of a large system size was performed to avoid spurious oscillations in the correlation functions introduced by the periodic boundary conditions. The large size was also preferred to access information—here and in future analysis—on the small wave-vector dynamical behavior.

In this paper we discuss in detail the autocorrelation function for the collective and self-density operators, both for center of mass (c.m.) and sites (s). The density operators ρ (and their corresponding autocorrelation functions) are defined as [37]

$$\rho_{c.o.m.}(\mathbf{q}) \equiv \frac{1}{\sqrt{N}} \sum_{i=1}^{N} e^{i\mathbf{q}\cdot\mathbf{r}^i_{c.o.m.}},$$

$$F_{c.o.m.}(\mathbf{q},t) \equiv \langle \rho_{c.o.m.}(\mathbf{q},t)\rho_{c.o.m.}(\mathbf{q},0)^* \rangle \tag{2}$$

$$\rho_s(\mathbf{q}) \equiv \frac{1}{\sqrt{3N}} \sum_{i=1}^{N} \sum_{j=1}^{3} e^{i\mathbf{q}\cdot\mathbf{r}^i_j}, \quad F_s(\mathbf{q},t) \equiv \langle \rho_s(\mathbf{q},t)\rho_s(\mathbf{q},0)^* \rangle, \tag{3}$$

$$\rho^{self}_{c.o.m.}(\mathbf{q}) \equiv e^{i\mathbf{q}\cdot\mathbf{r}^i_{c.o.m.}},$$

$$F^{self}_{c.o.m.}(\mathbf{q},t) \equiv \langle \rho^{self}_{c.o.m.}(\mathbf{q},t)\rho^{self}_{c.o.m.}(\mathbf{q},0)^* \rangle \tag{4}$$

$$\rho^{self}_s(\mathbf{q}) \equiv e^{i\mathbf{q}\cdot\mathbf{r}^i_j}, \quad F^{self}_s(\mathbf{q},t) \equiv \langle \rho^{self}_s(\mathbf{q},t)\rho^{self}_s(\mathbf{q},0)^* \rangle, \tag{5}$$

where $\mathbf{r}^i_{c.o.m.}$ and $\mathbf{r}^i_j$ are the position of the c.o.m. and of the j-site of molecule i. Moreover, $S_{c.o.m.}(q) \equiv F_{c.o.m.}(q,0)$ and $S_s(q) \equiv F_s(q,0)$ are the c.o.m. and site static structure factors.

We also present the l-dependent rotational correlators for the molecule symmetry axis $\boldsymbol{\mu}$, defined as

$$C_l(t) \equiv \langle P_l[\cos\theta(t)] \rangle, \tag{6}$$

where $\theta(t) = \cos^{-1}[\langle \boldsymbol{\mu}(t)\cdot\boldsymbol{\mu}(0)\rangle / \langle \boldsymbol{\mu}(0)\cdot\boldsymbol{\mu}(0)\rangle]$, and P_l is the l-order Legendre polynomial. The triplet site-site-site correlation function $c_3(\mathbf{k},\mathbf{p}\cdot\mathbf{q})$ defined as

$$\langle \rho_s(\mathbf{k})\rho_s(\mathbf{p})\rho_s(\mathbf{q}) \rangle = 3NS_s(k)S_s(p)S_s(q)$$
$$\times \delta_{\mathbf{q},\mathbf{k}+\mathbf{p}}[1 + n^2 c_3(\mathbf{k},\mathbf{p},\mathbf{q})] \tag{7}$$

has been calculated evaluating the left hand side of Eq. (7); n is the site number density. The evaluation of c_3 has been performed at $T = 266$ K, averaging over 1000 independent configurations, spanning a time interval of 75 ns. Where possible, up to 300 different triplets of wave vectors with the same moduli and relative angles have been averaged. We have calculated c_3 for moduli of $\mathbf{k}$, $\mathbf{p}$, and $\mathbf{q}$ less than 44.4 nm^{-1}, with a mesh of 0.44 nm^{-1}.

III. MODE COUPLING APPROXIMATIONS

In this paper we present two theoretical calculations of the site dynamics. The first approximation neglects completely the presence of the molecular constraints and assumes that the site-site structure factor includes all requested information on the structure of the liquid. This strong approximation allows to apply in a straightforward manner the MCT equation for simple liquids. According to MCT the time evolution of the normalized collective density correlation functions $\Phi_q(t)$ is given by

$$\ddot{\Phi}_q(t) + \nu_q\dot{\Phi}_q(t) + \Omega_q^2\Phi_q(t) + \Omega_q^2\int_0^t ds\, m_q(t-s)\dot{\Phi}_q(s) = 0. \tag{8}$$

Here $\Omega_q = \sqrt{qv/S_s(q)}$, with v denoting the thermal velocity, is an effective phonon-dispersion law and $\nu_q = \nu_o q^2$ denotes a damping constant. The kernel m_q is given as $m_q(t) = \mathcal{F}_q(\{\Phi_k(t)\})$, where the mode-coupling functional $\mathcal{F}_q$ is determined by the structure factor

$$\mathcal{F}_q(\{f_k\}) = \frac{1}{2}\int \frac{d^3k}{(2\pi)^3} V_{\mathbf{q},\mathbf{k}} f_k f_{|\mathbf{q}-\mathbf{k}|}, \tag{9}$$

$$V_{\mathbf{q},\mathbf{k}} \equiv S_s(q)S_s(k)S_s(|\mathbf{q}-\mathbf{k}|)\frac{n}{q^4}[\mathbf{q}\cdot\mathbf{k}c_k + \mathbf{q}\cdot(\mathbf{q}-\mathbf{k})c_{|\mathbf{q}-\mathbf{k}|}]^2, \tag{10}$$

where $c_q = [1 - S_s(q)^{-1}]/n$ is the direct correlation function in q space.

The second approximation is devised to retain some of the information of the molecular shape through the inclusion of the triplet correlation function c_3 [36], previously assumed to be zero. The vertex is then given by

$$V_{\mathbf{q},\mathbf{k}} \equiv S_s(q) S_s(k) S_s(|\mathbf{q}-\mathbf{k}|) \frac{n}{q^4}$$

$$\times [\mathbf{q}\cdot\mathbf{k} c_k + \mathbf{q}\cdot(\mathbf{q}-\mathbf{k}) c_{|\mathbf{q}-\mathbf{k}|} - q^2 n c_3(\mathbf{q},\mathbf{k},\mathbf{q}-\mathbf{k})]^2.$$

(11)

For simple atomic liquids, previous studies [36] showed that the approximation $c_3=0$ does not modify the MCT predictions, except for a small shift in the estimate of the critical temperature. Recently, it was shown [17] that in network forming liquids, the c_3 contributions play a crucial role. Including the c_3 contributions could, in the present case, be relevant for describing the intramolecular site-site relations. For this reason, we compare the numerical data with both predictions.

We numerically solved Eq. (8) on a grid of 300 equally spaced q values extending up to $q=120$ nm^{-1}, implementing the efficient techniques described in Ref. [38]. The long time limit of $\Phi_q(t)$ at the dynamical critical temperature—the so-called nonergodicity parameter f_q—is obtained by an iterative solution of the bifurcation equation

$$\frac{f_q}{1-f_q} = \mathcal{F}_q(\{f_k\}).$$

(12)

Close to the critical point, 20000 iterations were requested to solve Eq. (12) with a precision of 10^{-15}. We have solved Eq. (8) for both approximations. The estimated critical temperatures are $T=152$ and 340 K for the two approximations. Thus completely neglecting the molecular constraints (first approximation) strongly weakens the vertex function, resulting in a theoretical critical temperature lower than the numerical T_{MD}^c. Including the triplet correlation moves up the critical temperature by a factor larger than 2, resulting in an overestimation of the critical temperature, as always found in all previous MCT calculations. Notwithstanding the large difference in critical temperature the exponent parameter [15] is $\lambda=0.70$ in both approximations, corresponding to the exponents $b=0.64$ and $a=0.32$ [15].

In principle, one could also perform a MCT study based only on the center of mass structural information. In the present case, this is not feasible since, as it will be shown next, the c.o.m. structure factor does not depend on T in the region where slow dynamics develop, and hence there is no possibility to locate the ideal glass transition temperature. The MCT equations for simple liquids predict a liquid state if the T-independent $S_{c.o.m.}(q)$, together with the c.o.m. number density, are used as input in the theoretical calculations.

IV. MOLECULAR DYNAMICS RESULTS

A. Static

The site and c.o.m. static structure factors are shown in Fig. 1, as a function of temperature. The c.o.m. structure
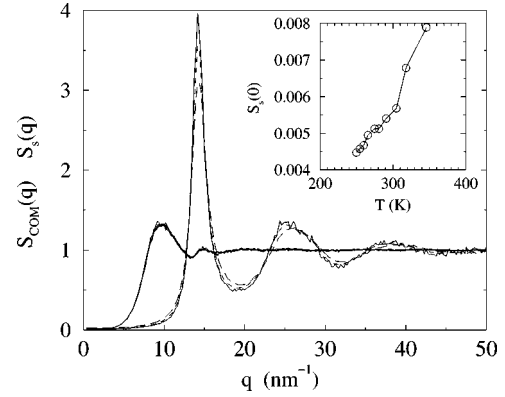

FIG. 1. $S_s(q)$ and $S_{c.o.m.}(q)$. For reasons of clarity, only data for $T=255$, 281, and 346 K are shown. Note that $S_{c.o.m.}(q)$ is temperature independent, while, for $S_s(q)$, the height of the first peak increases on cooling. The inset shows the T dependence of the structure factor at $q=0$.

factor does not show any appreciable change with T. Instead, the site structure factor increases significantly at the first peak position (corresponding in real space to the site-site nearest neighbor distance), consistently with the behavior of simple liquids. The absence of any change in the c.o.m. structure factor shows that the slowing down of the dynamics in this model is controlled by the changes in orientational order. It is the ordering process in the orientational degrees of freedom which drives the slowing down of the dynamics. Any theoretical approach attempting to predict the slow dynamics in this model must require orientational (or site-site) static information as input. The absence of any T dependence in the c.o.m. structure factor, except for the very clear reduction of the compressibility on cooling (see below), suggest the possibility that T-independent peaks in the experimentally measured OTP structure factor are associated with c.o.m. features. Of course, the present model does not allow a straightforward comparison with experimental data (as performed, for example, in Ref. [39]), since proton and carbon atoms are not explicitly taken into account. We note on passing that the T-independence of the c.o.m. static correlation is not a general feature of molecular liquids. In the case of simple point charge-extended (SPC/E), a model for water whose dynamics have been widely investigated [40,3,41], $S_{c.o.m.}(q)$ changes significantly in the supercooled region. Such changes play an important role in the slowing down of the molecular dynamics [18–20].

The large simulation box allows to precisely calculate the $q\rightarrow0$ limit of the structure factor. As expected, we find that $S_{c.o.m.}(q\rightarrow0)=S_s(q\rightarrow0)/3$. The T dependence of $S_s(q\rightarrow0)$ is shown in the inset of Fig. 1.

B. Self-dynamics

Figure 2 shows the T dependence of the diffusion coefficient D, evaluated from the long time behavior of the mean square displacement. Compared to the LW original data, the range of T where equilibrium states have been simulated is larger, and the precision in the determination of the values of D is improved. The larger T range shows that two regions, which differ in the T dependence of D, are observed. Above
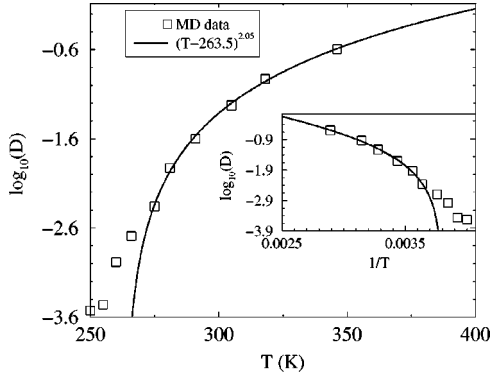
FIG. 2. Temperature dependence of the diffusion coefficient, evaluated from the long time limit of the mean square displacement. The inset shows the same data as a function of $1/T$.
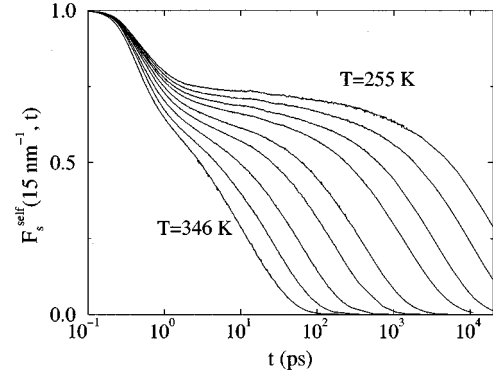

FIG. 3. Site self-correlation function for all studied temperatures at $q=15$ nm^{-1} (the location of the first maximum of the site structure factor).

$T=275$ K, $D(T)$ is consistent with a power law behavior in $T-T_{MD}^c$, with $T_{MD}^c=265\pm1$ K and exponent $\gamma=2.0\pm0.1$. Below $T=275$ K, D decreases at a slower pace, which could be approximated by an Arrhenius law. Hence, extending the simulation time by a factor 20 and the number of molecules by a factor 30 compared to the LW data, allows us to perform equilibrium simulations within the T region where deviations from the power-law behavior are observed. More specifically, as shown in Table I, a precise estimate of the diffusion coefficient is now possible down to 3.5 $\times 10^{-9}$ cm^2/s, a factor 20 smaller than the previous LW analysis [23].

The two different behaviors reflect the differences associated to the region of validity of MCT ($T>T_{MD}^c$) and to the region ($T<T_{MD}^c$), where hopping phenomena become relevant. The change in dynamical behavior shows up already for $|T-T_{MD}^c|/T_{MD}^c=0.06$, confirming the general expectation that hopping phenomena may mask the critical dynamics close to the critical MCT temperature. As discussed at length in Ref. [42], the presence of hopping phenomena in this model makes a clearcut identification of the critical dynamics impossible, without making use of information provided by the T dependence of the α-relaxation phenomenon. Similar changes in dynamical behavior close to the critical MCT temperature were recently reported in models of silica [43] and water [41]. It is worth noting that in the original work of LW, hopping phenomena in the orientational degrees of freedom were detected starting from $T=266$ K.

The temperature dependence of the site self-correlation function F_s^{self} is reported for a specific wave vector in Fig. 3. Similar figures characterize the time dependence of F_s^{self} at different values of q. The change in dynamics above and below T_{MD}^c can also be observed in the so-called time-T superposition graph, where curves for the same correlator are shown as a function of a scaled time. Indeed, in the α-relaxation region the so-called time-temperature superposition principle states that it is possible to represent the T dependence of an arbitrary correlator $\phi(t)$ on a single master curve, by rescaling the time via a single T-dependent time scale, i.e.,

$$\phi(t)=\phi(t/\tau(T)). \tag{13}$$

The scaling time $\tau(T)$ is conveniently defined [1] as the time when the correlation function has decayed to an arbitrary chosen value, for example $1/e$. Figure 4 shows the time-T superposition for the c.o.m. self-density correlation function both above and below (inset) T_{MCT}. Only for $T \geqslant 275$ K, where D is well described by a power law, is the time-T superposition principle well obeyed. Below 275 K, deviations start to be noticeable, and the plateau value starts to increase.

To describe the q dependence of the α relaxation in a compact way, and to make contact with the theoretical and experimental evaluations, in the next two figures we present parameters which better describe the self-density-density correlation functions according to the Von Schweidler law and the stretched exponential form. For a generic correlation function $\phi(t)$, the Von Schweidler law

$$\phi(t)=f_c-h_{(1)}(t/\tau)^b+h_{(2)}(t/\tau)^{2b}+O((t/\tau)^{3b}) \tag{14}$$

describes, including the next to leading order corrections, the departure from the plateau value f_c in the early α-relaxation region. The amplitudes $h_{(1)}$ and $h_{(2)}$ depend strongly on the physical features of the studied liquid, and were explicitly calculated within MCT for several models (see, for example,
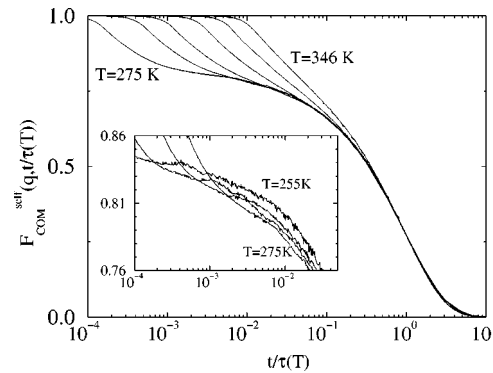

FIG. 4. α scaling for the c.o.m. self-correlation function for different T at $q=13$ nm^{-1}, the position of the first minimum of $S_{c.o.m.}(q)$. The main plot shows, from right to left, $T=346$, 318, 305, 291, 281, and 275 K. The inset shows the region around the plateau for $T=275$, 266, 260, and 255 K.
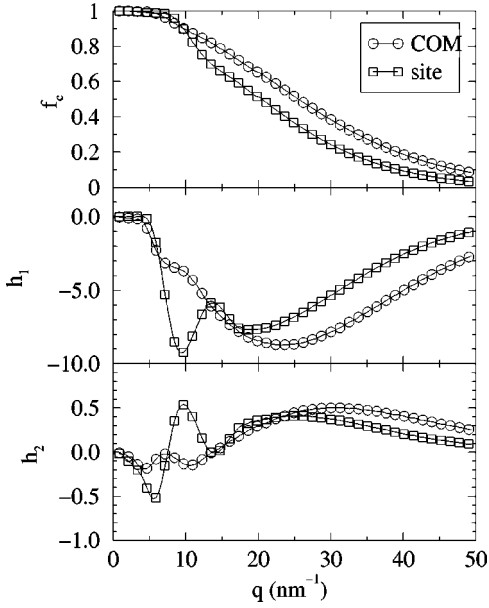
FIG. 5. Wave-vector dependence of the fitting parameters according to the Von Schweidler law [Eq. (14)] for the self-correlation functions $F_s^{self}(q,t)$ and $F_{c.o.m.}^{self}(q,t)$. $T = 275$ K. h_1 and h_2 are in arbitrary units.
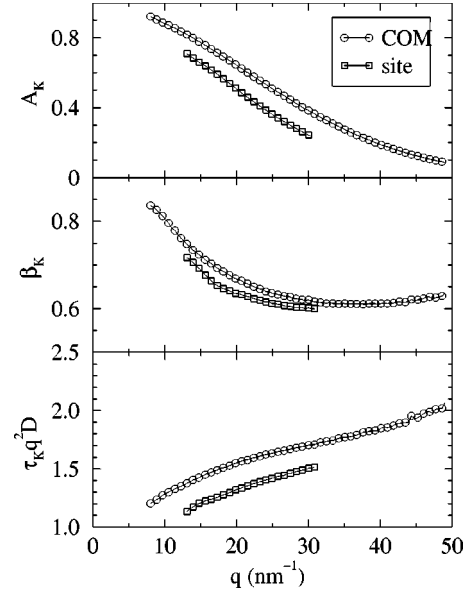

FIG. 6. Wave-vector dependence of the fitting parameters according to the stretched exponential form [Eq. (16)] for $F_s^{self}(q,t)$ and $F_{c.o.m.}^{self}(q,t)$. $T = 275$ K.

for hard spheres [44]). The α-relaxation time scale τ is a temperature dependent parameter which, according to MCT, scales as the inverse of diffusivity:

$$\tau(T) \sim |T - T_c|^{-\gamma}. \tag{15}$$

The exponent b is fixed by the value of γ [15]. The Kohlrausch-Williams-Watts stretched exponential form

$$\phi(t) = A_K e^{-(t/\tau_K)^{\beta_K}} \tag{16}$$

is often used to empirically fit the last part of the $\phi(t)$ decay.

Since all correlation functions obey the time-temperature superposition principle, the parameters of the two functional forms are calculated by fitting the $T = 275$ K correlation function in the time interval $30 < t < 600$ ps for the Von Schweidler law, and in the time interval $t > 20$ ps for the stretched exponential form. Similar results are obtained by fitting the $T = 266$ K data. The fit of the data according to Eq. (14) has been performed by constraining the exponent b to two different values: the value $b = 0.64$, obtained theoretically in Sec. III for both approximations and the value $b = 0.77$, consistent with the exponent γ extracted from the analysis of the diffusivity data. The fitting parameters f_c do not depend on the value of b. Except for a q-independent multiplicative factor, the q-dependence of h_1 is (within the errors) also independent of the choice of b.

Figure 5 shows the q dependence of the fitting parameters according to Eq. (14). In the case of the self-correlation function, the nonergodicity parameter $f_c(q)$ provides a description, in q space, of the confining cage. The width of the c.o.m. cage is larger than that of the site cage, supporting the view that the site experiences an additional delocalization associated with hindered librational motions. Moreover, we

note that the site nonergodicity parameter is not described by a simple Gaussian in q space. The q dependence of h_1 and h_2 follows the oscillation of the corresponding static structure factor.

Figure 6 shows the fitting parameters according to Eq. (16). At small wave vectors the extremely long decay of the correlation function, controlled by the diffusion of the molecules over distances of the order of q^{-1}, does not allow an unbiased determination of the fitting parameters. From the wave-vector range where the fitting parameters are reliable, one can note that, as commonly found, A_k mimics f_q, that β goes to 1 at small q, and that the product $Dq^2\tau$ has a weak q dependence.

We also report the rotational dynamics of the LW molecule along the symmetry axis. Figure 7(a) shows the time dependence of the first five Legendre polynomials. We also show the corresponding fit with the stretched exponential and the Von Schweidler law. For all angular correlators, the time-temperature superposition principle holds beautifully, as shown in Fig. 7(b). Since the quality of the data is very good, even tiny discrepancies would be visible. For completeness, we also report the fitting parameters according to the functional forms of Eqs. (14)–(16) in Figs. 8 and 9. The monotonic behavior of the fitting parameters in l suggests that for the LW potential, the scenario for the rotational dynamics is of the strong hindrance type [45], as found also for the case of SPC/E water [46,40]. This observation is consistent with the observed T independence of the static c.o.m. structure factor. The theoretical prediction of the wavevector dependence of the quantities reported in Figs. 5, 6, 8, and 9 is one of the major challenges to the recent proposed molecular mode coupling theories [47,32,33].

C. Collective dynamics

The collective density fluctuations are particularly relevant in the description of liquid dynamics. The nonmono-
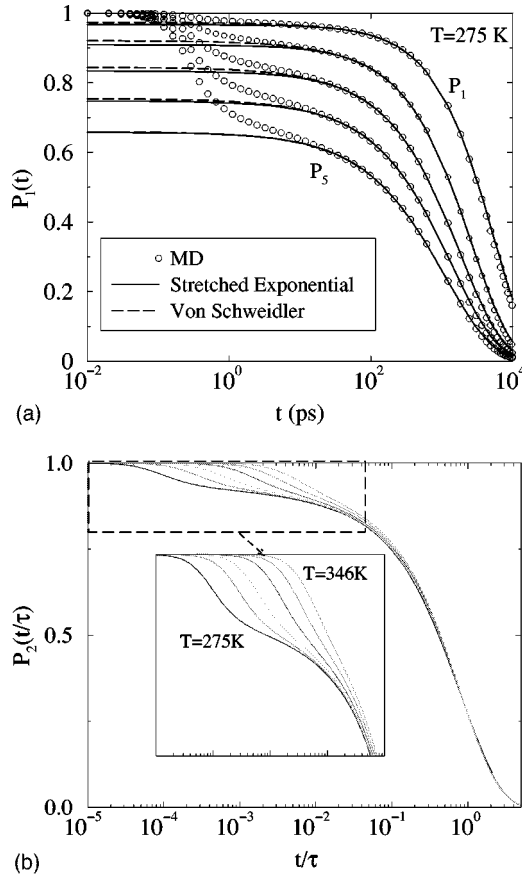
FIG. 7. (a) time dependence of the first five Legendre polynomials at $T=275$ K. (b) time-temperature superposition for the second-order Legendre polynomium.
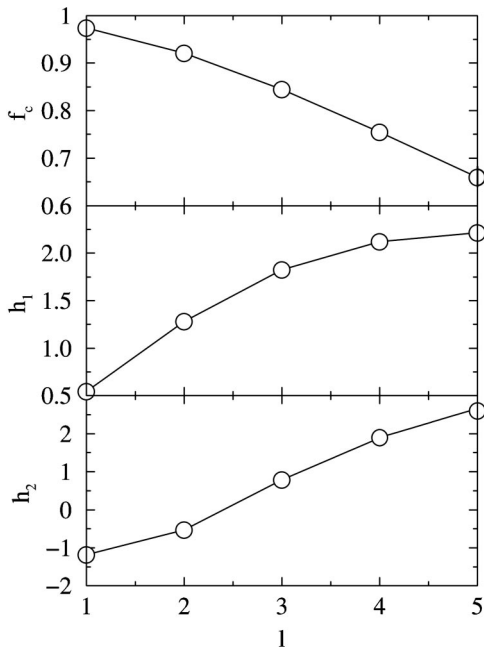

FIG. 8. Fitting parameters according to the Von Schweidler law of the first five Legendre polynomials. h_1 and h_2 are in arbitrary units.
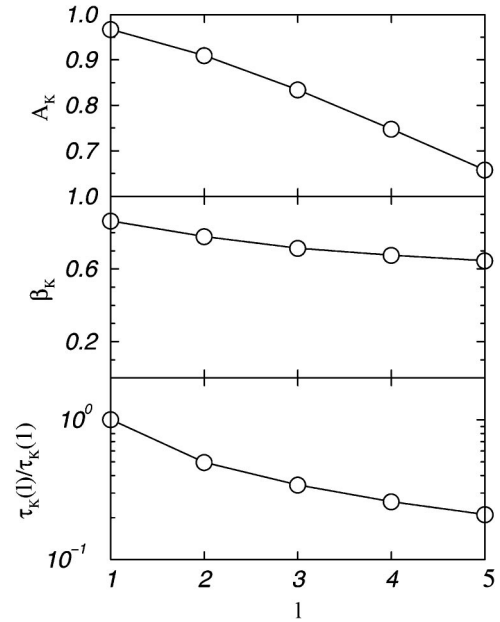

FIG. 9. Legendre order dependence of the fitting parameters according to the stretched exponential form [Eq. (16)].

tonic wave-vector dependence of the characteristic times provides an indication of the different time scales of the structural modes of the system, and their connection with the system characteristic lengths.

We start by discussing the site-site correlation functions, which can be compared with the corresponding correlation functions calculated according to MCT, as discussed in Sec. III. In comparing with the Von Schweidler and stretched exponential parametrizations, the solutions of the MCT equations (with and without the c_3 contribution), have been treated similarly to the MD data. Figure 10 shows the q dependence of the stretched exponential parameters A_K, β_K, and τ_K. We note that the theory captures the q dependence of the α-relaxation phenomenon close to the maximum of the site-site structure factor. The large wave-vector region is also described in a reasonable way. The theory fails in describing the nonergodicity parameters in the region where the c.o.m. structure factor has its peak position. The slowest modes in the system are indeed located around 9 nm^{-1} ($S_{c.o.m.}$ peak position) and around 15 nm^{-1} (S_s peak position). The role of the center of mass static correlation in controlling the molecular dynamics was observed in recent experimental studies on supercooled molecular liquids [48].

The slowing down of the dynamics in the very low-q region, below the region of influence of the c.o.m., is also predicted in a reasonable way by the site MCT developed in Sec. III. The stretching exponent parameter β_K is the one which seems to suffer more by the chosen approximations, which neglects site-site intramolecular constraints. Indeed, the theoretical estimate is always higher than the MD results. One tentative explanation for the higher value of β can be traced back to the reduced number of vertices included in the chosen MCT approach. Indeed, if the stretching phenomenon is considered to result from a distribution of decay times, then the addition of further coupling mechanisms in the
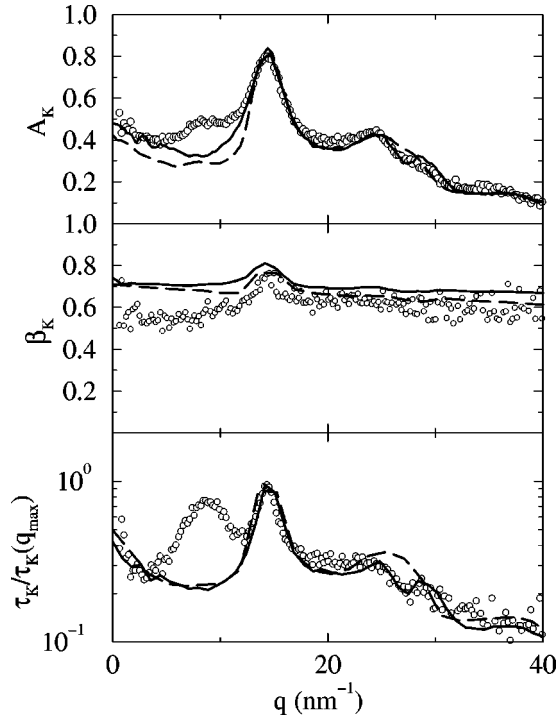
FIG. 10. Wave-vector dependence of the fitting parameters according to the stretched exponential form [Eq. (16)] for the normalized $F_s(q,t)$. Symbols are MD results. The full and dashed lines are the predictions of the MCT using the site structure factor as input, and including or excluding the c_3 contribution.

memory function might result in a wider distribution of decay times, and hence in a smaller stretching exponent. A more elaborate MCT approach would require as input a large number of angular static structure factor correlators [49] (which for the present molecule would make the theory difficult to solve numerically) or site-site partial static structure factors, discriminating at least between the central site and the two external sites. The development of the molecular and site-site MCT approaches is taking place at the present time,
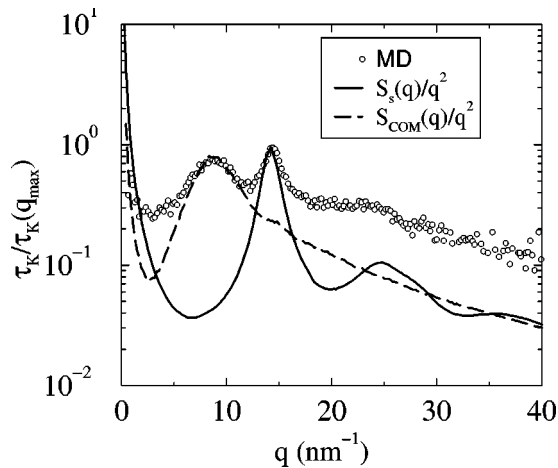

FIG. 11. Comparison of the wave-vector dependence of the α-relaxation time with the de Gennes approximation for both site and c.o.m.
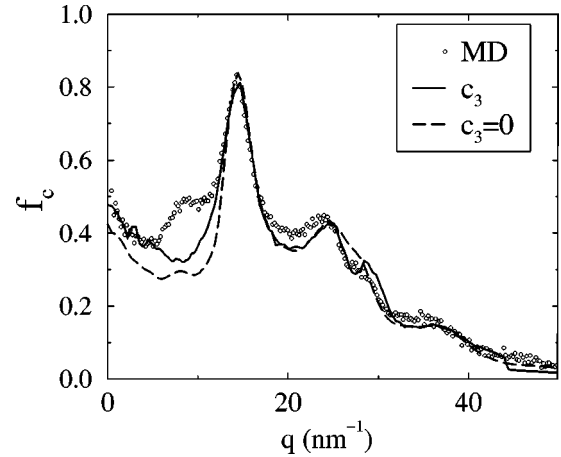

FIG. 12. Wave-vector dependence of the nonergodicity factor. The MD data were calculated as fitting parameters according to the Von Schweidler law [Eq. (14)]. The full and dashed lines are the prediction of MCT using the site structure factor as input, and including or excluding the c_3 contribution.

and we look forward to applying them to the LW model.

To substantiate the hypothesis that the disagreement between theory and MD data in the region around 9 nm^{-1} arises from the approximation used, which neglects the constraints among sites due to the intramolecular bonding, in Fig. 11 we compare the de Gennes predictions for the c.o.m. and site correlation times with the corresponding MD data (from Fig. 10). It is clearly seen that the dynamics in the wave-vector region around 9 nm^{-1} is indeed controlled by the c.o.m. static structure factor [50].

We next compare in Figs. 12 and 13 the prediction of MCT for the nonergodicity parameter, and for the amplitude of the Von Schweidler law with the MD results. Again, we note that the theoretical predictions satisfactorily describe the MD data except for the region where the c.o.m. structure factor has its maximum. Including the c_3 contribution improves the agreement in the hydrodynamic limit. Around the peak position of $S_s(q)$, the agreement is very good, consid-
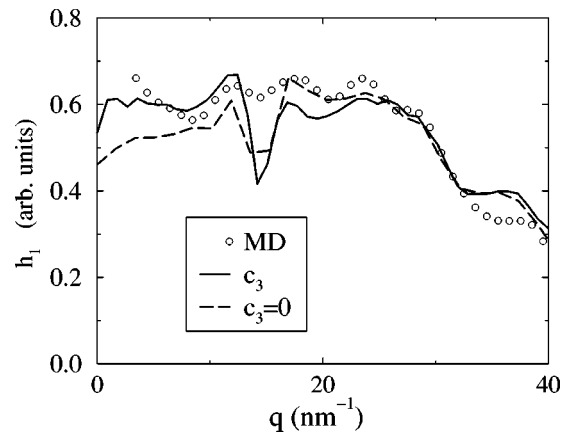

FIG. 13. Wave-vector dependence of the amplitude h_1 (in arbitrary units). The MD data (symbols) are the result of the fit according to the Von Schweidler law [Eq. (14)]. Lines are MCT predictions.
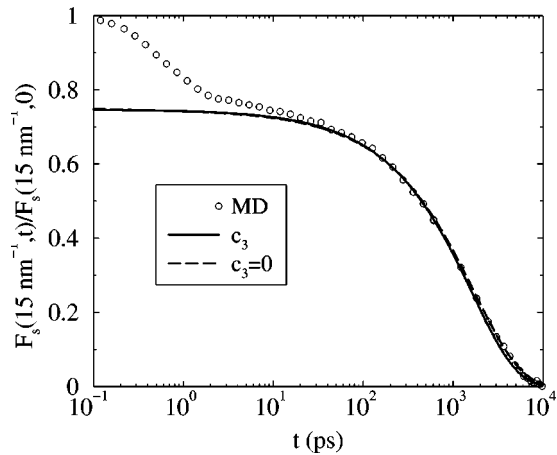
FIG. 14. Site-site α-relaxation dynamics at the peak of the structure factor. Symbols are MD results at $T=275$ K, and lines are MCT predictions for the α-relaxation dynamics close to the MCT critical temperature.

ering that neither fitting nor scaling parameters are involved in the comparison. In this wave-vector region, the long-time dependence of the collective site-site correlation function $F_s(q,t)$ is rather well predicted by the theory, as shown in Fig. 14.

We now turn to the c.o.m. correlators. These functions cannot be compared with the theoretical predictions reported in Sec. III, since this approximation neglects the molecular constraints. But the q dependence of the c.o.m. correlators is very relevant for comparisons with future molecular MCT predictions. Figures 15 and 16 show the parametrization of the c.o.m. collective α-relaxation using Eqs. (16) and (14).
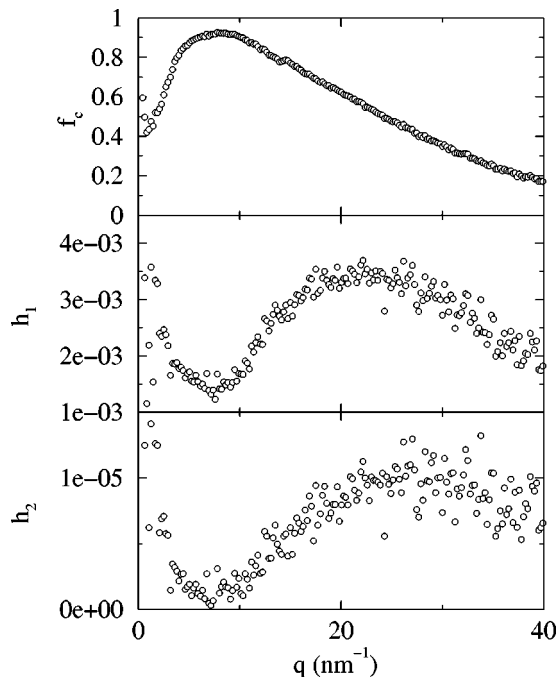

FIG. 15. Wave-vector dependence of the fitting parameters according to the stretched exponential form [Eq. (16)] for the normalized $F_{c.o.m.}(q,t)$.
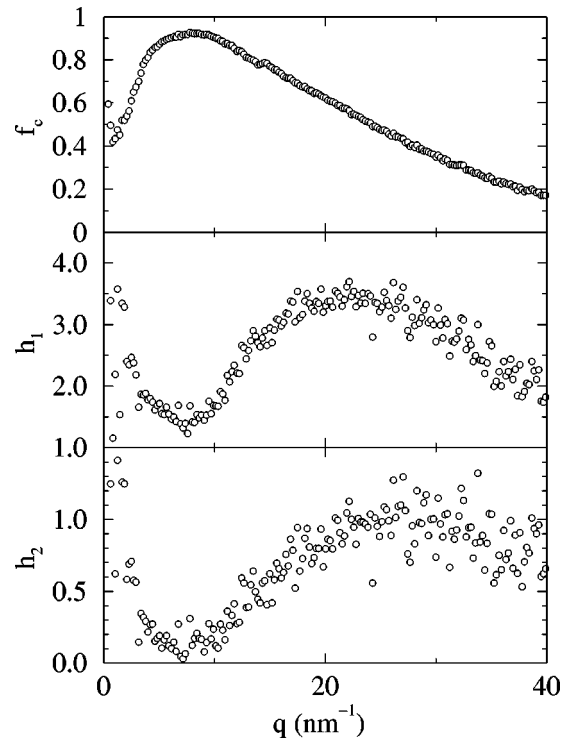

FIG. 16. Wave-vector dependence of the fitting parameters according to Eq. (14) for the normalized $F_{c.o.m.}(q,t)$. h_1 and h_2 are in arbitrary units.

The rather featureless shape of the c.o.m. structure, which, as seen in Fig. 1, shows only a broad peak around 9 nm^{-1}, carries on to the q dependence of all fitting parameters.

V. CONCLUSIONS

The present study of the simple molecular model introduced by Lewis and Wahnström to mimic the behavior of *ortho*-terphenyl provides a clean and simple reference model for theoretical descriptions of the dynamics of molecular liquids in supercooled states.

The MCT analysis reported in this paper, and compared in detail with the MD data, shows that MCT equations for atomic liquids are able to provide a rather accurate description of the site dynamics, except for the region around 9 nm^{-1} where the c.o.m. dynamics is dominant. We have provided evidence that, in this region, the center of mass fully controls the slow dynamics in the liquid [50]. We took into account that the triplet correlation function c_3 is shown to improve only the small wave-vector region significantly. This is not surprising, since the usually employed approximation $c_3=0$ fails badly at small wave vectors [51,52]. While this is not a major issue in the intermediate wave-vector range (i.e., for the caging physics) it will become an important element in the attempt to extend (toward long wavelengths) the theoretical predictions.

The present theoretical work, which can be considered a zeroth order approximation to the molecular description, should be followed by an accurate site-site MCT approach [32] or by a full molecular MCT approach [34]. Theoretical

developments along these two lines are taking place at a fast pace, and in the near future accurate theoretical predictions should be available for the quantities studied in this paper. For the present time, we can only state that the characteristic MCT scenario appears able to describe the dynamics of this simple, yet complete, molecular model.

[1] W. Kob and H. C. Andersen, Phys. Rev. E **51**, 4626 (1995); **52**, 4134 (1995).

[2] M. Nauroth and W. Kob, Phys. Rev. E **55**, 657 (1997).

[3] F. Sciortino, P. Gallo, P. Tartaglia, and S.-H. Chen, Phys. Rev. E **54**, 6331 (1996); P. Gallo, F. Sciortino, P. Tartaglia, and S.-H. Chen, Phys. Rev. Lett. **76**, 2730 (1996).

[4] F. Sciortino, L. Fabbian, S.-H. Chen, and P. Tartaglia, Phys. Rev. E **56**, 5397 (1997).

[5] M. C. Ribeiro and P. A. Madden, J. Chem. Phys. **108**, 3256 (1998), and references therein.

[6] B. Doliwa and A. Heuer, Phys. Rev. E **61**, 6898 (2000).

[7] S. K. Lai and G. F. Wang, Phys. Rev. E **58**, 3072 (1998).

[8] S. Kämmerer, W. Kob, and R. Schilling, Phys. Rev. E **56**, 5450 (1997).

[9] A. Heuer, Phys. Rev. Lett. **78**, 4051 (1997); S. Büchner and A. Heuer, Phys. Rev. E **60**, 6507 (1999).

[10] S. Sastri, P. Debenedetti, and F. Stillinger, Nature (London) **393**, 554 (1998).

[11] F. Sciortino, W. Kob, and P. Tartaglia, Phys. Rev. Lett. **83**, 3214 (1999); F. Sciortino and P. Tartaglia, *ibid.* **86**, 107 (2001).

[12] C. Donati, F. Sciortino, and P. Tartaglia, Phys. Rev. Lett. **85**, 1464 (2000).

[13] E. La Nave, A. Scala, F. W. Starr, F. Sciortino, and H. E. Stanley, Phys. Rev. Lett. **84**, 4605 (2000).

[14] L. Angelani, R. Di Leonardo, G. Ruocco, A. Scala, and F. Sciortino, Phys. Rev. Lett. **85**, 5356 (2000).

[15] W. Götze, in *Liquids, Freezing and Glass Transition*, edited by J. P. Hansen, D. Levesque, and J. Zinn-Justin, Les Houches Session LI, 1989 (North-Holland, Amsterdam, 1991).

[16] W. Götze, J. Phys.: Condens. Matter **11**, A1 (1999).

[17] F. Sciortino and W. Kob, Phys. Rev. Lett. **86**, 648 (2001).

[18] L. Fabbian, F. Sciortino, F. Thiery, and P. Tartaglia, Phys. Rev. E **57**, 1485 (1998).

[19] L. Fabbian, A. Latz, R. Schilling, F. Sciortino, P. Tartaglia, and C. Theis, Phys. Rev. E **60**, 5768 (1999).

[20] C. Theis, F. Sciortino, A. Latz, R. Schilling, and P. Tartaglia, Phys. Rev. E **62**, 1856 (2000).

[21] A. Winkler, A. Latz, R. Schilling, and C. Theis, Phys. Rev. E **62**, 8004 (2000).

[22] B. J. Alder and T. E. Wainwright, J. Chem. Phys. **27**, 1208 (1957).

[23] L. J. Lewis and G. Wahnström, Phys. Rev. E **50**, 3865 (1994).

[24] D. J. Plazek, C. A. Bero, and I. C. Chay, J. Non-Cryst. Solids **172-174**, 181 (1994).

[25] W. Petry, E. Bartsch, F. Fujara, M. Kiebel, H. Sillescu, and B. Farago, Z. Phys. B: Condens. Matter **83**, 175 (1991).

[26] J. Wuttke, M. Kiebel, E. Bartsch, F. Fujara, W. Petry, and H. Sillescu, Z. Phys. B: Condens. Matter **91**, 357 (1993).

[27] E. Bartsch, F. Fujara, J. F. Legrand, W. Petry, H. Sillescu, and J. Wuttke, Phys. Rev. E **52**, 738 (1995).

[28] A. Tölle, H. Schober, J. Wuttke, and F. Fujara, Phys. Rev. E **56**, 809 (1997).

[29] C. Masciovecchio, G. Monaco, G. Ruocco, F. Sette, A. Cunsolo, M. Krisch, A. Mermet, M. Soltwisch, and R. Verbeni, Phys. Rev. Lett. **80**, 544 (1998).

[30] G. Monaco, C. Masciovecchio, G. Ruocco, and F. Sette, Phys. Rev. Lett. **80**, 2161 (1998).

[31] G. Monaco, D. Fioretto, C. Masciovecchio, G. Ruocco, and F. Sette, Phys. Rev. Lett. **82**, 1776 (1999).

[32] S.-H. Chong and F. Hirata, Phys. Rev. E **58**, 6188 (1998); **58**, 7296 (1998); **57**, 1691 (1998).

[33] T. Franosch, M. Fuchs, W. Götze, M. R. Mayr, and A. P. Singh, Phys. Rev. E **56**, 5659 (1997).

[34] R. Schilling and T. Scheidsteger, Phys. Rev. E **56**, 2932 (1997); T. Scheidsteger and R. Schilling, Philos. Mag. B **77**, 305 (1998); C. Theis, Diploma thesis, Johannes Gutenberg Universität Mainz, 1997.

[35] G. Wahnström and L. J. Lewis, Prog. Theor. Phys. Suppl. **126**, 261 (1997).

[36] J.-L. Barrat, W. Götze, and A. Latz, J. Phys.: Condens. Matter **1**, 7163 (1989).

[37] J. P. Hansen and I. R. McDonald, *Theory of Simple Liquids*, 2nd ed. (Academic Press, London, 1986).

[38] A. P. Singh, Diploma thesis, TU München, 1995.

[39] S. Mossa, R. Di Leonardo, G. Ruocco, and M. Sampoli, Phys. Rev. E **62**, 612 (2000); S. Mossa, G. Ruocco, and M. Sampoli, preprint, cond-mat/0012474.

[40] F. Sciortino, Chem. Phys. **258**, 295 (2000).

[41] F. W. Starr, S. Harrington, F. Sciortino, and H. E. Stanley, Phys. Rev. Lett. **82**, 3629 (1999).

[42] F. Sciortino and P. Tartaglia, J. Phys.: Condens. Matter **11**, A261 (1999).

[43] J. Horbach and W. Kob, Phys. Rev. B **60**, 3169 (1999).

[44] M. Fuchs, I. Hofacker, and A. Latz, Phys. Rev. A **45**, 898 (1992).

[45] W. Gotze, A. P. Singh, and Th. Voigtmann, Phys. Rev. E **61**, 6934 (2000).

[46] L. Fabbian, F. Sciortino, and P. Tartaglia, J. Non-Cryst. Solids **235-237**, 350 (1998).

[47] C. Theis and R. Schilling, J. Non-Cryst. Solids **235-237**, 106 (1998).

[48] D. Morineau and C. Alba-Simionesco, J. Chem. Phys. **109**, 8494 (1998); D. Morineau, C. Alba-Simionesco, M. C. Bellissent-Funel, and M. F. Lautie, Europhys. Lett. **43**, 195 (1998).

[49] L. Fabbian, A. Latz, R. Schilling, F. Sciortino, P. Tartaglia, and C. Theis, Phys. Rev. E **62**, 2388 (2000).

[50] C. Alba-Simionesco, A. Tölle, D. Morineau, B. Farago, and G. Coddens, e-print cond-mat/0103599.

[51] The wave-vector dependence of the triplet density fluctuations $\langle \rho_s(\mathbf{k}) \rho_s(\mathbf{p}) \rho_s(\mathbf{q}) \rangle$ fully determines the wave-vector dependence of the static structure factor (i.e., the pair density fluctuations) via the Born-Green-Yvon (BGY) equation [52]. It is possible to show that the approximation $c_3 = 0$, when used in conjunction with the BGY equation, produces an implicit equation for the static structure factor which does not depend on density. The approximation $c_3 = 0$ should not be used in the hydrodynamic limit.

[52] N. H. March and M. P. Tosi, *Atomic Dynamics in Liquids* (Dover, New York, 1991), p. 23.